

# Phase Transitions, Hydrogen Bond and Crystal Dynamics of *p*-Methylbenzyl Alcohol as Studied by Single Crystal X-ray Diffraction and $^2\text{H}$ NMR

Masao Hashimoto, Michiko Harada, Motohiro Mizuno<sup>a</sup>, Masanori Hamada<sup>a</sup>, Tomonori Ida<sup>a</sup>, and Masahiko Suhara<sup>a</sup>

<sup>a</sup> Department of Chemistry, Faculty of Science, Kobe University, Nada-ku, Kobe 657-8501, Japan

<sup>b</sup> Department of Chemistry, Faculty of Science, Kanazawa University, Kanazawa, 920-1192, Japan

Reprint requests to Dr. M. H.; E-mail: mhashi@kobe-u.ac.jp

Z. Naturforsch. **57 a**, 381–387 (2002); received January 23, 2002

Presented at the XVIth International Symposium on Nuclear Quadrupole Interactions, Hiroshima, Japan, September 9-14, 2001.

The title compound (*p*MBA) was found to undergo a first-order phase transition at 211 K ( $T_{c1}$ ). Another transition with subtle enthalpy change appeared at 172 K ( $T_{c2}$ ). Crystal structure determinations at various temperatures revealed that the transition at  $T_{c1}$  was accompanied by remarkable changes in the molecular conformations around the  $\text{CH}_2\text{-C}$  and  $\text{O-CH}_2$  bonds and a reversal of the direction of the  $\text{O-H}\cdots\text{O}$  hydrogen bond. Experiments of  $^2\text{H}$  NMR were carried out on *p*MBA-d where the hydroxyl hydrogen of *p*MBA was selectively deuterated. Analyses of the  $^2\text{H}$  NMR spectra and the temperature dependence of  $T_1$  of the  $^2\text{H}$  NMR indicated occurrence of jumping motions of  $^2\text{H}$  between asymmetric potential wells at temperatures lower than  $T_{c1}$ .

**Key words:** Crystal Structure; Phase Transition;  $^2\text{H}$  NMR; Crystal Dynamics; Hydrogen Bond.

## Introduction

*p*-Methylbenzyl Alcohol (*p*MBA) is a homologue of *p*-chloro- and *p*-bromobenzyl alcohols (*p*ClBA and *p*BrBA respectively). The latter undergo first order phase transition at 236 K and 217 K, respectively [1, 2], and the crystal structure of the *p*ClBA at room temperature is known [3]. A higher order phase transition has been also proposed for *p*BrBA and *p*ClBA (at 195 and 218 K, respectively).

Recently we found that *p*MBA exhibits phase transitions bearing strong resemblance to those of *p*ClBA and *p*BrBA. In the present work we studied the crystal structure of *p*MBA at  $120 < T/\text{K} < 260$  by single crystal X-ray diffraction. Moreover, we investigated the dynamics of the hydrogen atoms in the  $\text{O-H}\cdots\text{O}$  hydrogen bond network by means of  $^2\text{H}$  NMR on *p*MBA-d, where the hydroxyl hydrogen of *p*MBA was selectively deuterated. The  $^2\text{H}$  NMR spectrum and spin-lattice relaxation time ( $T_1$ ) of  $^2\text{H}$  NMR will be discussed.

## Experimental

*p*MBA, obtained from nacalai tesque, was recrystallized from *n*-hexane several times to purify the material. Single crystals suitable for the X-ray work were crystallized from an ethanol-water mixed solution of *p*MBA. For  $^2\text{H}$  NMR measurements, the hydroxyl hydrogen of *p*MBA was selectively deuterated by  $\text{D}_2\text{O}$  in a dioxane solution to give *p*MBA-d. The degree of deuteration was checked by  $^1\text{H}$  NMR of *p*MBA-d dissolved in  $\text{CDCl}_3$ : no appreciable peak of  $^1\text{H}$  NMR from the hydroxyl proton was found.

Thermal analysis was carried out using differential scanning calorimeters (Rigaku DSC 8058 and MAC Science DSC 3100S).

Details of the single crystal X-ray experiment on *p*MBA are summarized in Table 1. The structure was solved by the direct method and refined by the full matrix least squares method with SHELXL-97 [4]. In the refinements of the crystal structure at 120 and 233 K non-hydrogen atoms were included in the least

Table 1. Crystal data and experimental details\*.

	C <sub>8</sub> H <sub>10</sub> O	
	120 K	233 K
Formula	C <sub>8</sub> H <sub>10</sub> O	
Formula weight	122.16	
Temperature	120 K	233 K
Crystal system	monoclinic	monoclinic
Space group	<i>P</i> 2 <sub>1</sub>	<i>P</i> 2 <sub>1</sub>
<i>a</i> /Å	14.576(2)	14.560(3)
<i>b</i> /Å	4.854(1)	4.935(1)
<i>c</i> /Å	15.017(2)	15.023(3)
$\beta$	107.103(3)	105.993(3)
<i>V</i> /Å <sup>3</sup>	1015.5(3)	1037.6(3)
<i>Z</i>	6	6
<i>D<sub>x</sub></i> / g·cm <sup>-3</sup>	1.199	1.173
$\mu$ (Mo K $\alpha$ )/mm <sup>-1</sup>	0.077	0.076
<i>F</i> (000)	396	396
Crystal dimensions	0.57×0.33×0.20 mm <sup>3</sup>	
Radiation	graphite monochromated Mo-K $\alpha$	
<i>R</i> ( <i>F</i> <sub>o</sub> <sup>2</sup> )/[ <i>I</i> > 2 $\sigma$ ( <i>I</i> )]	0.0495	0.0677
<i>R<sub>w</sub></i> ( <i>F</i> <sub>o</sub> <sup>2</sup> )	0.0417	0.0520
No. of reflection	3592	3200
No. of parameters	364	356
$\theta$ <sub>max</sub>	27.5°	27.5°
( $\Delta/\sigma$ ) <sub>max</sub>	0.000	0.000
( $\Delta/\rho$ ) <sub>max</sub> /e Å <sup>-3</sup>	0.179	0.444
( $\Delta/\rho$ ) <sub>min</sub> /e Å <sup>-3</sup>	-0.228	-0.240
Diffractometer	BRUKER SMART 1000	
Weighting	$w = 1/[\sigma^2(F_o^2) + c_1P + (c_2P)^2]$ ,	
scheme	$P = (F_o^2 + 2F_c^2)/3$	
<i>c</i> <sub>1</sub> ; <i>c</i> <sub>2</sub>	0; 0.0724	0.0439; 0.0949

\* Crystal data at various temperatures have been deposited in CCDC under the deposition numbers CCDC 170083 - 170086.

squares calculations with anisotropic thermal parameters. All of the hydrogen atoms were included in the refinement with isotropic thermal parameters without constraints. But for the structure at 233 K, two hydrogen atoms belonging to a CCH<sub>2</sub> group were included in the calculations with constraints.

The <sup>2</sup>H NMR spectra were measured by using a CMX-300 spectrometer at 45.825 MHz. A ( $\pi/2$ )<sub>x</sub>- $\tau$ -( $\pi/2$ )<sub>y</sub>- $\tau$ -acquisition pulse sequence was used. The  $\pi/2$  pulse width and  $\tau$  were 3.0 and 30  $\mu$ s, respectively. *T*<sub>1</sub> was determined by the saturation-recovery and inversion-recovery methods.

## Results and Discussion

### Phase Transitions

Thermal analysis of *p*MBA evidenced a first-order phase transition at 211 K (*T*<sub>c1</sub>). The enthalpy of the transition ( $\Delta H$ ) was 1.0 kJ/mol. In addition we found a small but evident peak of the DSC curve whose on-set

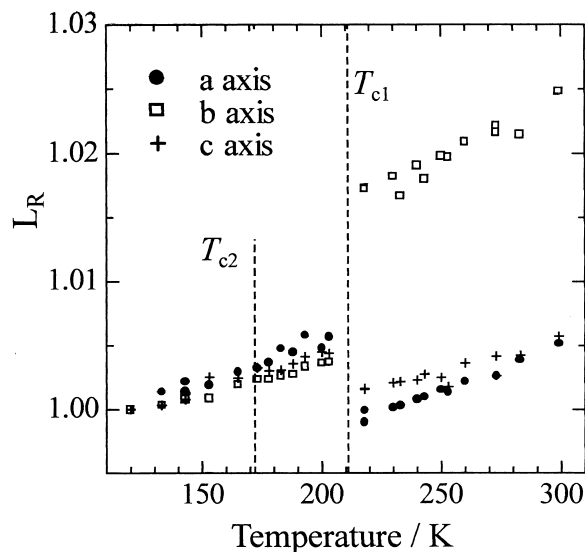


Fig. 1. Temperature dependence of the unit cell length (*a*, *b* and *c*) given by relative values (*L<sub>R</sub>*): *L<sub>R</sub>* = *L*(*T*)/*L*(120), where *L*(*T*) is the unit cell length of the *a*, *b*, or *c* axis at *T*/K.

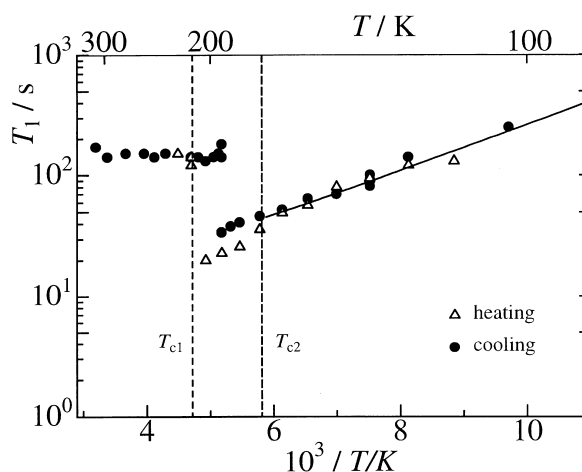


Fig. 2. Temperature dependence of *T*<sub>1</sub> of <sup>2</sup>H NMR.

temperature was 172 K (*T*<sub>c2</sub>). Although its enthalpy change was subtle (ca. 0.03 kJ/mol), it is an indication of a phase transition. The results of the thermal analysis on *p*MBA-d agreed with those of *p*MBA, except for the fact that the thermal anomaly at *T*<sub>c2</sub> was broad. In this paper, the relevant phases are tentatively referred to as low, intermediate and room temperature phases (LTP, ITP and RTP, respectively).

Figure 1 shows the temperature dependence of the unit cell constants of *p*MBA. Discontinuous changes appearing at *T*<sub>c1</sub> can be ascribed to a first order phase

Table 2. Atomic coordinates and equivalent thermal parameters ( $U_{\text{eqv}}/\text{\AA}^3$ ) at 120 and 233 K.

Atom	— at 120 K —				— at 233 K —			
	<i>x</i>	<i>y</i>	<i>z</i>	$U_{\text{eqv}}$	<i>x</i>	<i>y</i>	<i>z</i>	$U_{\text{eqv}}$
Molecule A:								
C11	0.34871(12)	0.7069(4)	0.13447(12)	0.0193(4)	0.85081(16)	−0.0190(7)	0.14054(18)	0.0413(7)
C12	0.38621(13)	0.7960(5)	0.22610(12)	0.0238(4)	0.88921(19)	0.0722(8)	0.23038(18)	0.0466(8)
C13	0.46090(12)	0.9850(5)	0.24969(12)	0.0244(4)	0.96245(18)	0.2607(8)	0.2502(2)	0.0476(8)
C14	0.50126(12)	1.0895(4)	0.18341(13)	0.0235(5)	0.99996(17)	0.3619(7)	0.18203(18)	0.0417(7)
C15	0.46325(12)	1.0005(5)	0.09178(12)	0.0228(4)	0.96099(18)	0.2739(7)	0.09241(18)	0.0451(8)
C16	0.38798(12)	0.8128(5)	0.06787(12)	0.0228(4)	0.88758(18)	0.0874(8)	0.07195(18)	0.0453(8)
C17	0.27008(13)	0.4952(5)	0.10670(13)	0.0225(4)	0.7741(2)	−0.2278(8)	0.1164(3)	0.0555(10)
C18	0.58129(14)	1.2977(5)	0.20905(15)	0.0278(5)	1.0788(2)	0.5694(8)	0.2047(3)	0.0532(9)
O11	0.20171(9)	0.5120(4)	0.15705(9)	0.0246(3)	0.70021(13)	−0.1702(5)	0.15639(15)	0.0603(6)
H11	0.1712(17)	0.667(6)	0.1421(17)	0.053(8)	0.667(4)	−0.358(16)	0.176(4)	0.19(2)
Molecule B:								
C21	0.18313(12)	0.5628(4)	0.46690(12)	0.0201(4)	0.31578(16)	0.3461(8)	0.52874(17)	0.0393(7)
C22	0.22473(12)	0.4643(5)	0.55674(12)	0.0222(4)	0.27489(19)	0.2505(7)	0.44102(18)	0.0450(8)
C23	0.29976(13)	0.2751(5)	0.57419(13)	0.0254(4)	0.20138(18)	0.0642(8)	0.42422(19)	0.0485(8)
C24	0.33552(12)	0.1801(4)	0.50370(13)	0.0223(5)	0.16689(17)	−0.0343(7)	0.4956(2)	0.0441(8)
C25	0.29322(13)	0.2798(5)	0.41373(12)	0.0244(4)	0.20837(19)	0.0640(8)	0.58357(19)	0.0491(8)
C26	0.21831(12)	0.4675(5)	0.39573(12)	0.0215(4)	0.28206(18)	0.2521(7)	0.60063(18)	0.0459(8)
C27	0.10344(13)	0.7733(5)	0.44603(12)	0.0207(4)	0.3935(2)	0.5544(8)	0.5483(2)	0.0492(8)
C28	0.41521(14)	−0.0305(5)	0.52282(16)	0.0300(5)	0.0883(2)	−0.2414(9)	0.4779(3)	0.0589(10)
O21	0.04649(9)	0.7631(3)	0.50843(9)	0.0237(3)	0.45752(15)	0.5094(6)	0.49642(17)	0.0651(7)
H21	0.0152(18)	0.591(5)	0.5015(18)	0.044(7)	0.487(3)	0.667(8)	0.497(2)	0.061(10)
Molecule C:								
C31	0.97921(12)	0.2067(4)	0.18791(12)	0.0192(4)	0.52405(17)	−0.0166(7)	0.8172(2)	0.0476(8)
C32	0.93145(12)	0.3129(5)	0.10041(12)	0.0223(4)	0.5708(2)	0.0872(8)	0.9022(2)	0.0523(8)
C33	0.85719(12)	0.5001(5)	0.09000(12)	0.0233(4)	0.64289(19)	0.2760(8)	0.91178(19)	0.0524(9)
C34	0.82763(12)	0.5876(4)	0.16572(13)	0.0219(4)	0.67074(17)	0.3652(7)	0.83568(17)	0.0416(7)
C35	0.87528(12)	0.4781(5)	0.25285(12)	0.0220(4)	0.62375(19)	0.2585(8)	0.75060(18)	0.0482(8)
C36	0.95003(12)	0.2911(5)	0.26370(12)	0.0222(4)	0.55145(19)	0.0725(8)	0.74174(19)	0.0510(8)
C37	1.05856(12)	−0.0026(5)	0.20130(12)	0.0208(4)	0.4471(2)	−0.2254(9)	0.8033(2)	0.0709(11)
C38	0.74866(14)	0.7969(5)	0.15413(15)	0.0261(4)	0.7479(3)	0.5699(9)	0.8461(3)	0.0529(9)
O31	1.10783(9)	0.0114(3)	0.13245(8)	0.0238(3)	0.38279(16)	−0.1674(7)	0.8511(2)	0.0741(8)
H31	1.1374(16)	0.173(5)	0.1421(16)	0.036(7)	0.356(3)	−0.319(10)	0.858(2)	0.086(14)

transition, while the existence of a phase transition at  $T_{c2}$  seems ambiguous in this figure.

Figure 2 shows the temperature dependence of  $T_1$  of  $^2\text{H}$  NMR. The  $\log(T_1)$  vs.  $1/T$  curve on heating shows an abrupt increase in  $T_1$  at  $T_{c1}$ , corresponding to the transition from ITP to RTP. It is difficult, however, to assign the discontinuous decrease in  $T_1$  observed at ca. 193 K on cooling to the transition from RTP to ITP, since the values of  $T_1$  on cooling are significantly longer than those on heating in the temperature range between  $T_{c2}$  and 193 K. An idea to interpret this discrepancy, depending on thermal history, is the assumption that RTP transforms into a metastable state on cooling. It would be a superheated state of LTP, because values of  $T_1$  obtained on cooling in the temperature range mentioned above

coincide with those extrapolated from LTP. The values of  $T_1$  obtained on heating are considered to be representative of ITP. A break in the  $\log(T_1)$  vs.  $1/T$  curve appeared at around  $T_{c2}$  corresponding to the transition from LTP to ITP.

### Crystal Structure

The crystal system and the space group of the three modifications, LTP, ITP and RTP were found to be identical. The crystal structure of *p*MBA at 120 K is illustrated in Figure 3. The asymmetric unit contains three kinds of crystallographically independent *p*MBA molecules (denoted as molecule A, B and C). Molecules A and C belong to the same antipode, while

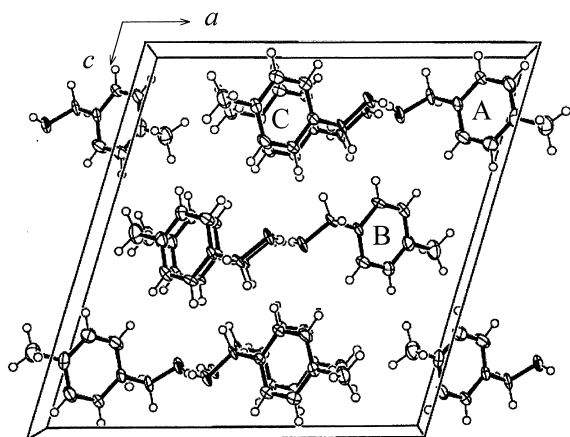
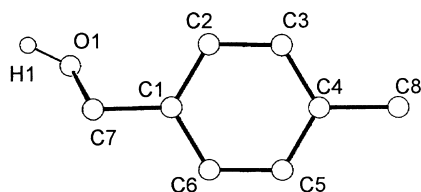


Fig. 3. Crystal structure of *p*MBA at 120 K projected on the *ac* plane. The notations A, B and C are used to distinguish three crystallographically independent molecules.

B to opposite one. The atomic coordinates and equivalent thermal parameters at 120 K (LTP) and 233 K (RTP) are given in Table 2. The atomic numbering scheme is:



Such notations as C17, C27 and C37, for instance, are also used to distinguish the C7 atoms in molecule A, B and C, respectively.

As shown in Fig. 3 the molecules B form infinite O-H...O hydrogen bonded chains along the  $2_1$  axes (Chain 1), while the molecules A and C form another kind of chains related by a pseudo  $2_1$  axis along the *b* axis (Chain 2). The two kinds of hydrogen-bonded chains in LTP and RTP are illustrated in Fig. 4 (a) and (b).

The temperature dependence of the dihedral angle O1-C7-C1-C2 ( $\chi$ ) for the molecules A, B and C are shown in Figure 5. Discontinuous increases in  $\chi$  by ca. 11, 8 and 15 degrees were observed at  $T_{c1}$  for molecule A, B and C, respectively. It is evident that the phase transition at  $T_{c1}$  is accompanied by a remarkable change in the molecular conformation around the C7-C1 bond of each molecule. Furthermore, it should be noted that the  $\chi$ 's of molecule B and C are markedly temperature dependent in RTP.

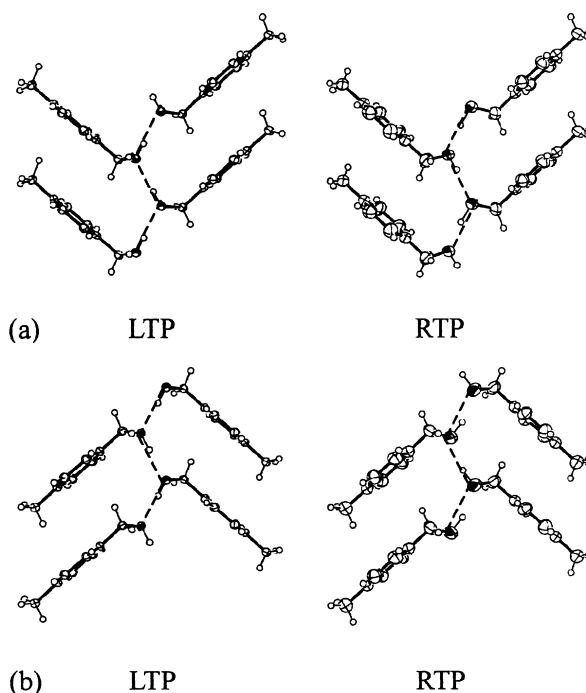


Fig. 4. Hydrogen bonded chains of *p*MBA molecules in LTP and RTP. (a) Chain 1 formed by molecules B along a  $2_1$  axis; (b) Chain 2 formed by molecules B and C related by a pseudo  $2_1$  axis along the *b* axis.

The angles between the C2-C6 vector of each molecule and the three crystal axes were found to be almost constant over the temperature range investigated and exhibit quite small changes (ca.  $1^\circ$ ) at  $T_{c1}$ . The same feature was observed for the angles between the C1-C4 vector and the three crystal axes. These facts indicate that the orientation of the benzene ring is substantially independent of temperature, leading to the conclusion that the jump of  $\chi$  at  $T_{c1}$  can be attributed to a displacement of the oxygen atom.

In the hydrogen bond chains illustrated in Fig. 4, the intermolecular O...O distances were found to show slight discontinuities (less than 0.03 Å) at  $T_{c1}$ . This observation indicates that the hydrogen bond chains shift as a whole like a 'micro piston' along the crystal *b* axis as the phase transition takes place.

As can be seen from Fig. 4 (a) and (b), the direction of the O-H...O hydrogen bond in Chain 1 is opposite to that in Chain 2. Furthermore, it is interesting that the direction of the O-H...O hydrogen bond in RTP is opposite to that in LTP, both in Chain 1 and 2. It should be noted that the hydroxyl hydrogen atom is located on a *trans* position with respect to the benzene

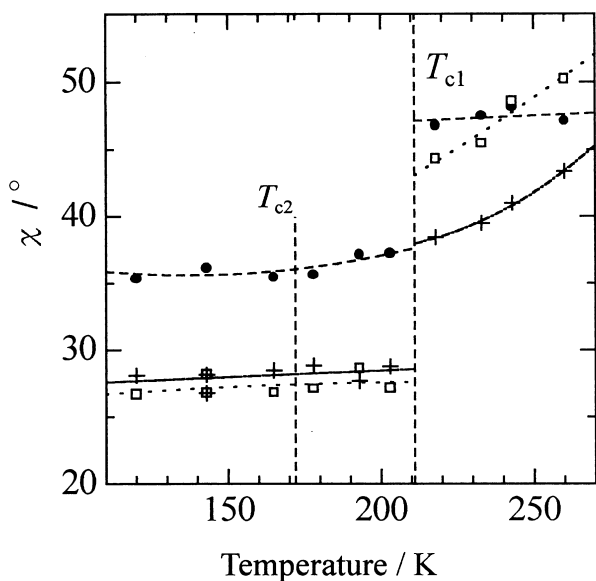


Fig. 5. Temperature dependence of the O1-C7-C1-C2 dihedral angle ( $\chi$ ) of each *p*MBA molecule. Filled circles, crosses and open squares correspond to molecule A, B and C, respectively. The lines are guides to eyes.

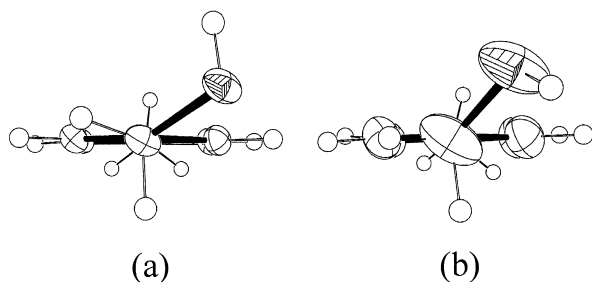


Fig. 6. ORTEP drawings of molecule A: (a) in LTP (at 120 K) and (b) in RTP (at 233 K).

ring in LTP and ITP, while *cis* in RTP (Fig. 6). This conformational change seems to be favorable for the reversal of the direction of the hydrogen bond. As to the mechanism of the reversal of the hydrogen bond, there are, in general, two possibilities, that is, conformational and configurational ones [5]. The former seems favorable in the present case.

#### Analyses of the Results of $^2\text{H}$ NMR

##### $^2\text{H}$ NMR in LTP

The central feature of the  $^2\text{H}$  NMR spectrum at 158 K (LTP) shown in Fig. 7, indicates the existence

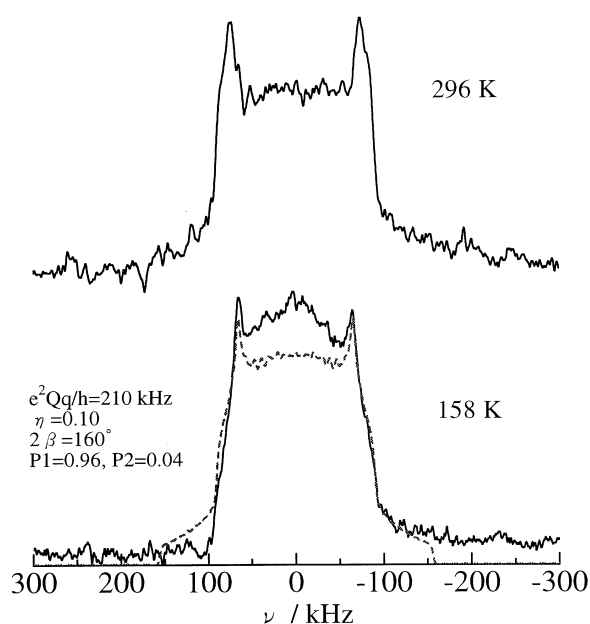


Fig. 7.  $^2\text{H}$  NMR spectra. Top and bottom for RTP and LTP, respectively. The broken line in the bottom spectrum is the simulated one (for details, see the text).

of a fast local motion. Distribution of the proton site would also contribute to produce the central feature. However, this contribution may be neglected because the spectrum of RTP has no evident central feature. As can be seen in Fig. 2,  $T_1$  in LTP decreases exponentially with increasing temperature. In order to analyze these results we assumed a jumping motion of the hydroxyl hydrogen atom (D) between two asymmetric potential wells, illustrated schematically in Fig. 8(a). For the sake of simplicity, the difference between the OH groups of molecules A, B and C were neglected.

The  $^2\text{H}$  NMR spectrum at 158 K could be reproduced by the following parameters: quadrupole coupling constant ( $e^2Qq/h$ ) = 210 kHz, asymmetric parameter ( $\eta$ ) = 0.1 and the D...O...D angle ( $2\beta$ ) =  $160^\circ$ . This value of  $2\beta$  suggests that the two proton sites (site 1 and 2 in Fig. 8(a)) correspond approximately to the positions of the hydroxyl hydrogen atoms in RTP and LTP.

The fluctuation of the electric field gradient at the  $^2\text{H}$  nucleus caused by the jumping motion of the hydrogen atom is considered to dominate  $T_1$ . If one neglects the small  $\eta$  of 0.1,  $T_1$  is expressed by [6, 7]

$$T_1^{-1} = \frac{1}{10} \frac{4a}{(1+a)^2} \left( \frac{3e^2Qq}{4\hbar} \right)^2 (\sin 2\beta)^2 \quad (1)$$

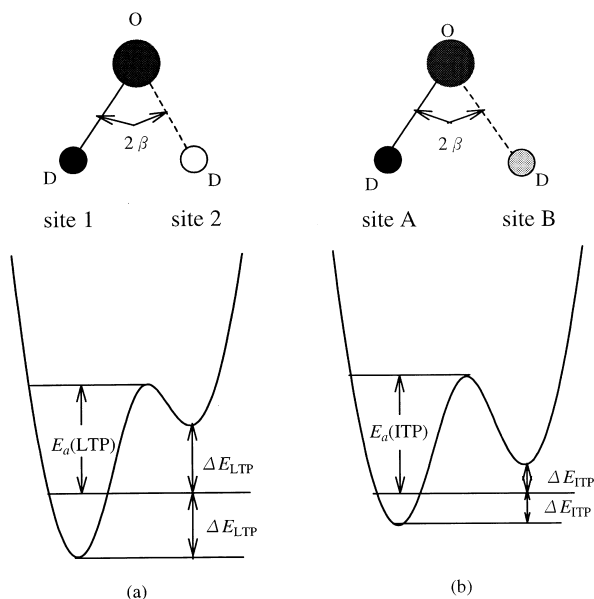


Fig. 8. Models of the potential governing the motion of the hydroxyl hydrogen (D) atom.

$$\cdot \left\{ \frac{\tau_c}{1 + \omega_0^2 \tau_c^2} + \frac{4\tau_c}{1 + 4\omega_0^2 \tau_c^2} \right\},$$

$$a = \exp\left(\frac{2\Delta E}{RT}\right), \quad (2)$$

$$\tau_c = (1 + a)^{-1} \tau_{c0} \exp\left(\frac{E_a + \Delta E}{RT}\right), \quad (3)$$

where  $\omega_0$ ,  $\tau_{c0}$  and  $E_a$  are the angular NMR frequency, correlation time at infinite temperature and activation energy for the jump of the hydroxyl D atom, respectively. As can be seen from Fig. 8,  $\Delta E$  is a measure of the deviation from symmetric potential wells. From the temperature dependence of  $T_1$ , values of  $E_a$  and  $\Delta E$  were calculated as  $(2.5 \pm 0.1)$  and  $(2.1 \pm 0.1)$  kJ/mol, respectively, by assuming that  $\Delta E = 0$  at  $T_{c1}$  and by using the magnitudes of  $e^2 Qq/h$  and  $2\beta$  estimated from the analysis of the  $^2\text{H}$  NMR spectrum.

#### $^2\text{H}$ NMR in ITP

The slope of the  $\log(T_1)$  vs.  $1/T$  curve in ITP is significantly different from that in LTP (Fig. 2). However, the potential model for the analysis of the behavior of  $T_1$  in ITP is expected to be quite similar to that for

LTP, because a minute structural difference is suggested by the extremely small magnitude of  $\Delta H(T_{c2})$ . Then for ITP, we adopted a potential curve shown in Fig. 8(b), which has the same parameters as those of LTP but with  $\Delta E$  smaller than that in LTP. The latter assumption indicates that the potential is less asymmetric than that for LTP. The choice of this potential model for ITP implies to examine the possibility that a higher order phase transition would be involved in the reversal of the hydrogen bond direction due to the transition from ITP to RTP.

For the parameters in (1), (2) and (3), except for  $\Delta E$ , we applied the values obtained for LTP and estimated the magnitude of  $\Delta E$ . It was found that  $\Delta E$  became lower with increasing temperature ( $2.0 \pm 0.1$ ) and  $(1.8 \pm 0.1)$  kJ/mol at 173 and 203 K, respectively. The value of  $\Delta E$  of ITP is comparable to that of LTP in the vicinity of  $T_{c2}$ , but, at higher temperatures of ITP it becomes appreciably lower than that of LTP. The tendency of decreasing  $\Delta E$  with increasing temperature found in ITP may be regarded as the initiation process of the phase transition from ITP to RTP, because the site B in Fig. 8(b), which approximately corresponds to the hydrogen position in RTP, is more populated at higher temperatures within ITP.

#### $^2\text{H}$ NMR in RTP

As can be seen in Fig. 6, the thermal ellipsoids for O1 and C7 atoms are considerably larger than those of the other atoms, suggesting an oscillation of the OH group around the C7-C1 bond. Moreover, the O1-C7-C1-C2 dihedral angles of the molecules B and C are significantly temperature dependent. These observations suggest that the hydroxyl hydrogen atom is in a force field that is strongly temperature dependent. As can be seen in Fig. 2,  $T_1$  in RTP is apparently temperature independent. Although this behavior is interesting, a detailed analysis of this phenomenon will be deferred until the temperature dependence of the potential curve dominating the motion of the hydrogen atom is known by further studies.

#### Acknowledgements

The authors would like to express appreciation to Professor K. Yamamura of Kobe University for the preparation of *p*MBA-d. This work was supported in part by a Grant-in-Aid for Scientific Research (No. 13640579) from the Ministry of Education, Science and Culture, Japan.

- [1] H. Niki, K. Kano, and M. Hashimoto, *Z. Naturforsch.* **51a**, 731 (1996).
- [2] M. Hashimoto, Y. Monobe, H. Terao, H. Niki, and M. Mano, *Z. Naturforsch.* **53a**, 436 (1998).
- [3] M. Hashimoto, Y. Nakamura, and K. Hamada, *Acta Cryst.* **C44**, 482 (1988).
- [4] G. M. Scheldrick, "SHELXL-97, Program for the Refinement of Crystal Structures", Univ. Goettingen, Germany 1997.
- [5] G. A. Jeffrey, "An Introduction to Hydrogen Bonding", Oxford University Press, Oxford 1997, Chapt. 7.
- [6] K. Morimoto, K. Shimomura, and M. Yoshida, *J. Phys. Soc. Japan* **52**, 3927 (1983).
- [7] M. Mizuno, Y. Hamada, T. Kitahara, and M. Sahara, *J. Phys. Chem. A* **103**, 4981 (1999).